more, Gls1p-HA was undetectable in COPII vesicles derived from *tip20-8* membranes (fig. S3). We also tested for homotypic fusion of COPII vesicles derived from Δ*gls1 TIP20* and *tip20-8 GLS1* membranes, which could in principle account for the trimmed [^{35}S]gpαF. Although as observed before [^{35}S]gpαF was trimmed, when COPII vesicles were incubated with *tip20-8* SICS, they did not undergo homotypic vesicle fusion (Fig. 4D, compare lanes 2 and 5). Furthermore, the SNARE and cargo composition of the COPII vesicles derived from *tip20-8* membranes was identical to that from wild-type or *tip20-5* membranes (fig. S3). Thus, back-fusion was not because of a sorting defect at ER exit sites.

Thus, our results suggest that there is an active mechanism that prevents back-fusion of transport vesicles to their donor membranes. We propose that Tip20p acts as a sensor for vesicles at the ER membrane. The nature of the interaction between Tip20p and the vesicle is still elusive. Tip20p recognizes either protein or lipid factors on the naked vesicle or the coat itself. The latter possibility seems more likely, because *tip20* displays genetic interaction with mutants in multiple coatomer subunits (*19*). Directionality in vesicular transport might thus be brought about at least in part by prohibiting back-fusion to the donor membrane.

References and Notes

1. R. Schekman, L. Orci, *Science* **271**, 1526 (1996).
2. J. E. Rothman, F. T. Wieland, *Science* **272**, 227 (1996).
3. H. R. Pelham, *Exp. Cell Res.* **247**, 1 (1999).
4. S. Springer, A. Spang, R. Schekman, *Cell* **97**, 145 (1999).
5. A. Spang, R. Schekman, *J. Cell Biol.* **143**, 589 (1998).
6. P. P. Poon *et al.*, *EMBO J.* **18**, 555 (1999).
7. A. Spang, J. M. Herrmann, S. Hamamoto, R. Schekman, *Mol. Biol. Cell* **12**, 1035 (2001).
8. D. J. Sweet, H. R. Pelham, *EMBO J.* **12**, 2831 (1993).
9. B. A. Reilly, B. A. Kraynack, S. M. VanRheenen, M. G. Waters, *Mol. Biol. Cell* **12**, 3783 (2001).
10. M. J. Lewis, J. C. Rayner, H. R. Pelham, *EMBO J.* **16**, 3017 (1997).
11. P. Cosson *et al.*, *Eur. J. Cell Biol.* **73**, 93 (1997).
12. U. Andag, T. Neumann, H. D. Schmitt, *J. Biol. Chem.* **276**, 39150 (2001).
13. A. Peyroche, S. Paris, C. L. Jackson, *Nature* **384**, 479 (1996).
14. The Golgi morphology was investigated also by electron microscopy and by Sec7p-GFP.
15. X. Cao, N. Ballew, C. Barlowe, *EMBO J.* **17**, 2156 (1998).
16. M. Latterich, R. Schekman, *Cell* **78**, 87 (1994).
17. M. Latterich, K. U. Frohlich, R. Schekman, *Cell* **82**, 885 (1995).
18. C. Barlowe, *J. Cell Biol.* **139**, 1097 (1997).
19. G. Frigerio, *Yeast* **14**, 633 (1998).

20. We are grateful to P. Cosson, J. Gerst, B. Glick, R. Schekman, and H.-D. Schmitt for strains and reagents. I. Macara and M. Trautwein are acknowledged for critical reading of the manuscript. This work was supported by the Max Planck Society. A.S. is an European Molecular Biology Organization Young Investigator.

Supporting Online Material

www.sciencemag.org/cgi/content/full/304/5668/286/DC1
Materials and Methods
Figs. S1 to S3
Table S1
References

23 December 2003; accepted 5 February 2004

Transmembrane Segments of Syntaxin Line the Fusion Pore of Ca^{2+}-Triggered Exocytosis

Xue Han, Chih-Tien Wang, Jihong Bai, Edwin R. Chapman, Meyer B. Jackson*

The fusion pore of regulated exocytosis is a channel that connects and spans the vesicle and plasma membranes. The molecular composition of this important intermediate structure of exocytosis is unknown. Here, we found that mutations of some residues within the transmembrane segment of syntaxin (Syx), a plasma membrane protein essential for exocytosis, altered neurotransmitter flux through fusion pores and altered pore conductance. The residues that influenced fusion-pore flux lay along one face of an α-helical model. Thus, the fusion pore is formed at least in part by a circular arrangement of 5 to 8 Syx transmembrane segments in the plasma membrane.

The manner in which lipids and proteins cooperate in the trafficking of cellular membranes remains poorly understood, despite the identification of many molecules with membrane trafficking functions. In regulated exocytosis, vesicle fusion proceeds through a stable intermediate structure known as the fusion pore. The existence of fusion pores was anticipated by the observation of reversal events in single-vesicle capacitance recordings (*1*) and was then demonstrated by combined capacitance-current measurements (*2*),

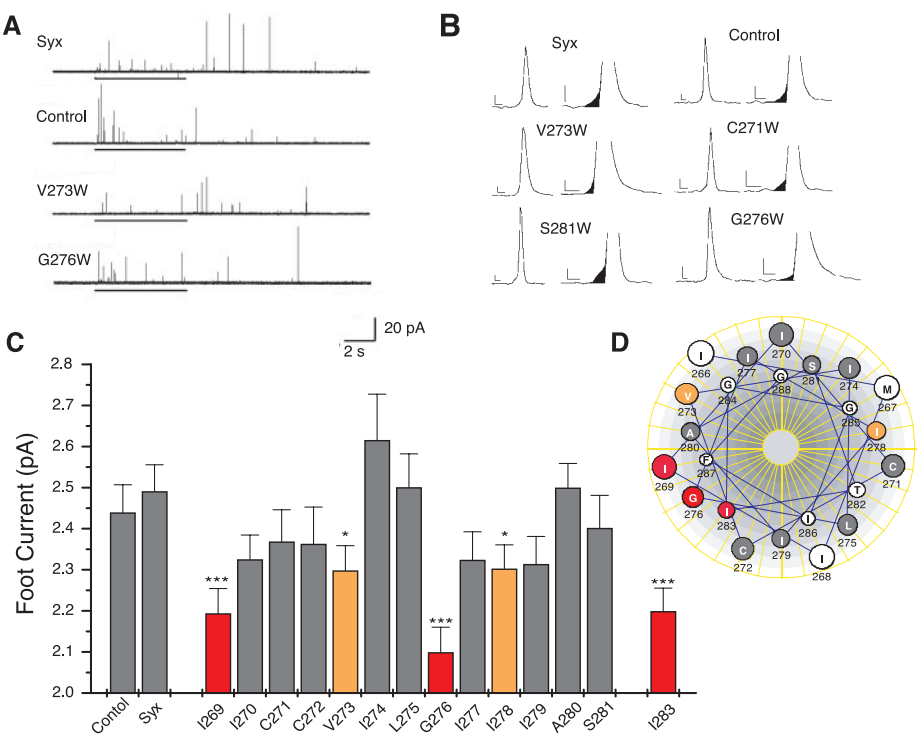

Fig. 1. Amperometry recordings from PC12 cells. (**A**) KCl depolarization (indicated by bars below each trace) elicits norepinephrine release. Single vesicle release events register as spikes from cells transfected with wild-type Syx, the control vector, and two Syx mutants. (**B**) Spikes were preceded by PSF. Expanded traces (right) show the PSF (shaded regions) in traces from Syx, the control, and four mutants. Scale bars, 5 pA and 1 ms. (**C**) The mean PSF amplitude was significantly reduced in five of the mutants tested. *, $P < 0.05$; ***, $P < 0.001$ for a Student's t test compared with the results of wild-type Syx; pooled values were used (195 to 432 PSF from 24 to 62 cells in 4 to 14 transfections). All values with $P < 0.001$ by the t test on the pooled mean were also significantly different ($P < 0.05$ for I269W and I283W; $P < 0.01$ for G276W) on the basis of the t test on the double mean (*26*). Error bars show the mean + SEM. (**D**) A helical wheel model [produced with DNAStar (DNASTAR Inc., Madison, WI)] placed the three locations 269, 276, and 283 with the strongest effects on the same face of an α helix. Color coding reflects the level of significance for pooled means (C). Open circles were not tested.

combined capacitance-conductance measurements (*3*), amperometry (*4*), and combined amperometry-capacitance measurements (*5*). Fusion pores in exocytosis often open abruptly, have apparent diameters comparable to those of large ion channels, and are stable for times ranging from milliseconds to seconds (*6*). No membrane flows between the vesicle and plasma membrane through the initial exocytic fusion pore (*7*). The fusion pore thus resembles a gap junction channel formed by an association between proteins in the vesicle and plasma membranes. However, there is no direct evidence that the fusion pore is composed of protein, and a lipidic fusion pore cannot be ruled out.

Manipulations are being discovered that can modulate fusion-pore stability. High extracellular Ca^{2+} promotes fusion-pore closure (*8*). Genetic ablation of the synaptosome-associated protein of 25 kD (SNAP-25) reduces fusion-pore stability (*9*). Different isoforms (*10*, *11*) and mutants (*12*) of the putative Ca^{2+} sensor for exocytosis, synaptotagmin, change the fusion-pore lifetime. These results imply that these proteins interact with the fusion pore in some way, but they do not identify the pore-forming molecules. Synaptotagmin binds the lipid and a number of proteins, in both Ca^{2+}-dependent and -independent manners (*13*), so regulation by this protein provides little information about the molecular composition of the fusion pore.

Ion channel gating is regulated by an extraordinarily diverse constellation of molecules (*14*–*16*). By contrast, ion flux through a channel is uniquely sensitive to the pore-lining residues of a channel-forming protein (*17*, *18*). Mutations that alter the charge or size of side chains along the ion permeation pathway can markedly alter the current through a channel. Thus, the flux through a fusion pore should also be sensitive to changes in its pore-lining constituents. With this rationale, we searched for protein domains that line the fusion pore. We selected the protein syntaxin (Syx) for the following reasons: (i) Syx is essential for exocytosis, as demonstrated by genetic ablation (*19*) and by the action of clostridial neurotoxins that cleave Syx (*20*). (ii) Among the proteins essential for exocytosis, Syx is the only plasma membrane protein with a membrane-spanning segment (*21*, *22*). (iii) Syx is the only neuronal target-soluble *N*-ethylmaleimide–sensitive factor attachment protein receptor (t-SNARE) with a transmembrane segment that is necessary for reconstitution of proteoliposome fusion (*23*). As an initial test of the hypothesis that the transmembrane segment of Syx lines the fusion pore, we performed tryptophan scanning and used amperometric measurements of fusion-pore flux to determine whether the open fusion pore is obstructed.

Amperometry detects norepinephrine as it is released from the rat neuroendocrine PC12 cell line (*24*). The release of a single vesicle registered as a spike of amperometric current (Fig. 1A), but a fusion pore opened ~1 ms before the spike to produce a prespike foot (PSF) (*4*) (Fig. 1B). The PSF amplitude provides a signal closely related to the norepinephrine flux through the fusion pore. PSF amplitudes were measured from PC12 cells transfected with mutants of Syx in which a native amino acid was replaced by tryptophan. We tested positions 269 to 281 and 283 in the membrane-spanning segment at the C terminus of Syx. Most transfections, including those with wild-type Syx and the control vector, produced PSF with average amplitudes in the range of 2.3 to 2.6 pA. However, tryptophan replacement of isoleucine 269 [$I^{269}\rightarrow W^{269}$ (I269W) (*25*)], glycine 276 (G276W), and isoleucine 283 (I283W) produced highly significant ($P < 0.001$) reductions in PSF amplitude (Fig. 1C) (*26*). V273W and I278W had smaller reductions that were also significant ($P < 0.05$).

A reduction in PSF amplitude would place a residue in the lining of the fusion pore so that its side chain can protrude into the pore lumen and interfere with norepinephrine flux. The residues with the largest effects (269, 276, and 283) fall along the same face of an α helix (Fig. 1D). Residue 273 is near this face. Residue 278 falls on a very different face of the helix, but one or two false positives at the $P < 0.05$ level is reasonable for 14 measurements. Thus, the Syx membrane-spanning segment forms an α helix, and the fusion pore is formed by a circular arrangement of several such segments.

Mutations that reduced PSF amplitude had no effect on current through voltage-activated Ca^{2+} channels (*24*) (Fig. 2, A to C) or on the Ca^{2+}-dependent association of Syx with synaptotagmin I (*24*) (Fig. 2D). The expression of Syx was determined by immunoblot analysis (Fig. 2E). With reference to the standards, the amount of wild-type Syx and G276W could be estimated as three times as great as the amount of endogenous Syx in control cells. Because 30% of the cells in the culture were transfected (*24*), the expression level in individual transfected cells increased ~10-fold. Thus, the transfected protein was the predominant form of Syx in the cells from which recordings were made.

To examine the effect of side-chain size further, a series of mutants was prepared at selected locations. For positions 269, 276, and 283, increasing side-chain volume produced a graded reduction in PSF amplitude (Fig. 3, A, C, and E), as expected for pore-lining residues. For positions 280 and 275, the plots were flat (Fig. 3, B and D), consistent with the notion that these were not pore-lining residues and did not interfere with norepinephrine flux through the fusion pore.

To evaluate fusion-pore obstruction by a different method, we used a lock-in amplifier to measure the complex impedance of membrane patches (*24*). These measurements revealed the fusion of single vesicles

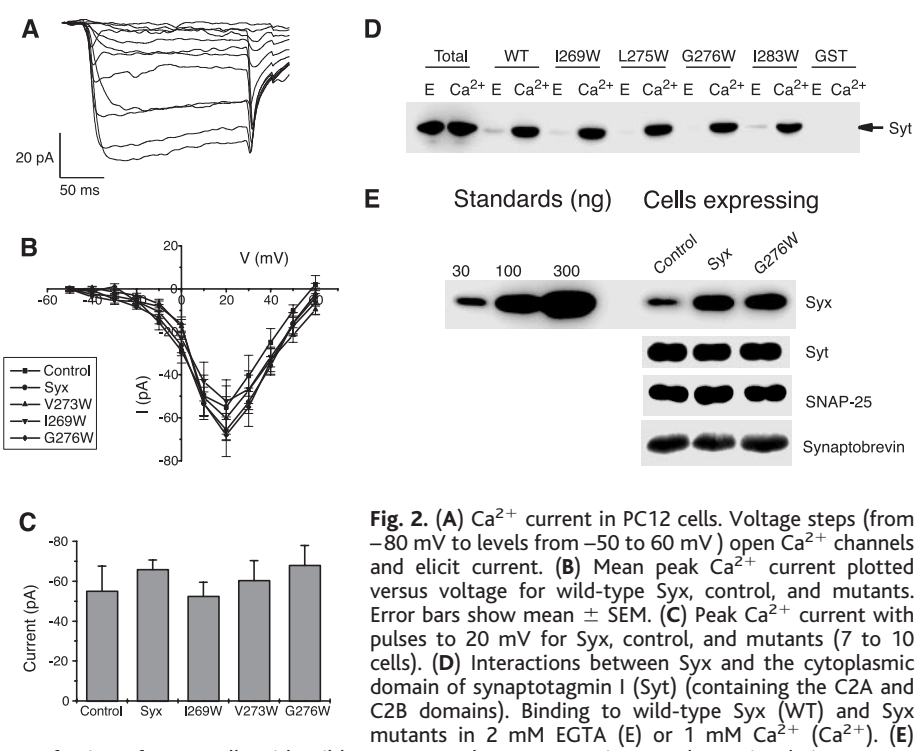

Fig. 2. (**A**) Ca^{2+} current in PC12 cells. Voltage steps (from −80 mV to levels from −50 to 60 mV) open Ca^{2+} channels and elicit current. (**B**) Mean peak Ca^{2+} current plotted versus voltage for wild-type Syx, control, and mutants. Error bars show mean ± SEM. (**C**) Peak Ca^{2+} current with pulses to 20 mV for Syx, control, and mutants (7 to 10 cells). (**D**) Interactions between Syx and the cytoplasmic domain of synaptotagmin I (Syt) (containing the C2A and C2B domains). Binding to wild-type Syx (WT) and Syx mutants in 2 mM EGTA (E) or 1 mM Ca^{2+} (Ca^{2+}). (**E**) Transfection of PC12 cells with wild-type Syx and Syx G276W increased Syx signals in Western blots of PC12 cell membranes by threefold over control cells. Expression levels of other proteins, Syt, SNAP-25, and synaptobrevin/VAMP were unchanged.

Department of Physiology, University of Wisconsin, 1300 University Avenue, Madison, WI 53706, USA.

*To whom correspondence should be addressed. E-mail: mjackson@physiology.wisc.edu

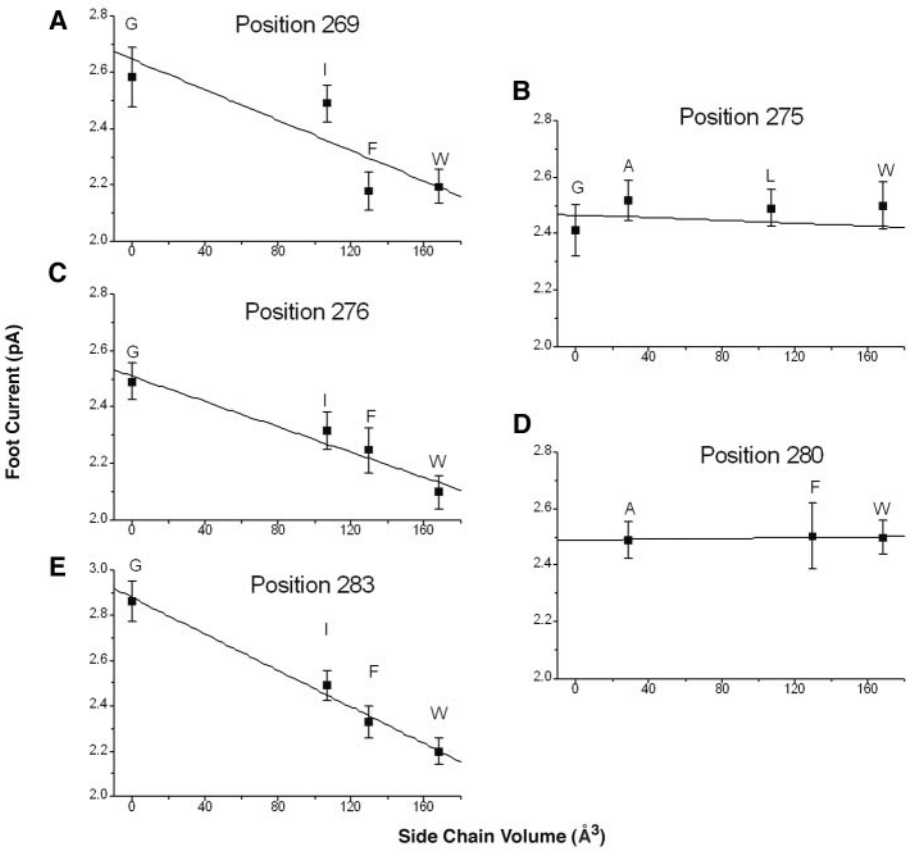

Fig. 3. Relation between PSF amplitude and side-chain volume. Substitutions at positions 269 (**A**), 276 (**C**), and 283 (**E**) produced graded reductions in PSF amplitude that increased with side-chain volume. The plots include the tryptophan mutants of Fig. 1. Plots for substitutions at positions 275 (**B**) and 280 (**D**) show no reduction with side-chain volume. All points are means of 183 to 432 events. Error bars show means ± SEM. Best-fitting lines were drawn through each plot. Letters identify the amino acid present at the indicated position (*25*). *P* values for no correlation were 0.19 (A), 0.58 (B), 0.03 (C), 0.32 (D), and 0.007 (E).

as stepwise changes in membrane capacitance (Fig. 4A). During the capacitance steps, it was sometimes possible to resolve transient changes in membrane conductance, from which the fusion-pore conductance can be calculated (*3*) (Fig. 4B). We selected two mutations that altered the PSF amplitude (I269W and G276W) and one that did not (L275W) for these more difficult experiments. All the mutants produced capacitance steps of ~0.2 fF (corresponding to an 84-nm vesicle diameter), which were indistinguishable from those seen with wild-type Syx (Fig. 4C). The average values varied by <5% and were statistically indistinguishable, indicating that none of the mutants altered vesicle size. The two mutants that reduced PSF amplitude also reduced the fusion-pore conductance by a factor of ~2, but the mutation that did not alter PSF amplitude had no effect on conductance (Fig. 4D). Thus, mutations that reduced norepinephrine flux also reduced ion current through open fusion pores. The larger reduction in conductance compared with PSF amplitude may indicate that inorganic ion flow is more sensitive to tryptophan obstruction than is the flow of the organic cation norepinephrine. Alternatively, the difference may reflect a difference in the population of fusion pores detected with the lock-in amplifier.

At least three residues of the membrane-spanning segment of Syx were thus placed in the lining of the fusion pore of Ca^{2+}-triggered exocytosis. The three residues with the largest effects fall on the same face of an α helix, whereas residues that fail to influence fusion-pore flux faced away. We can

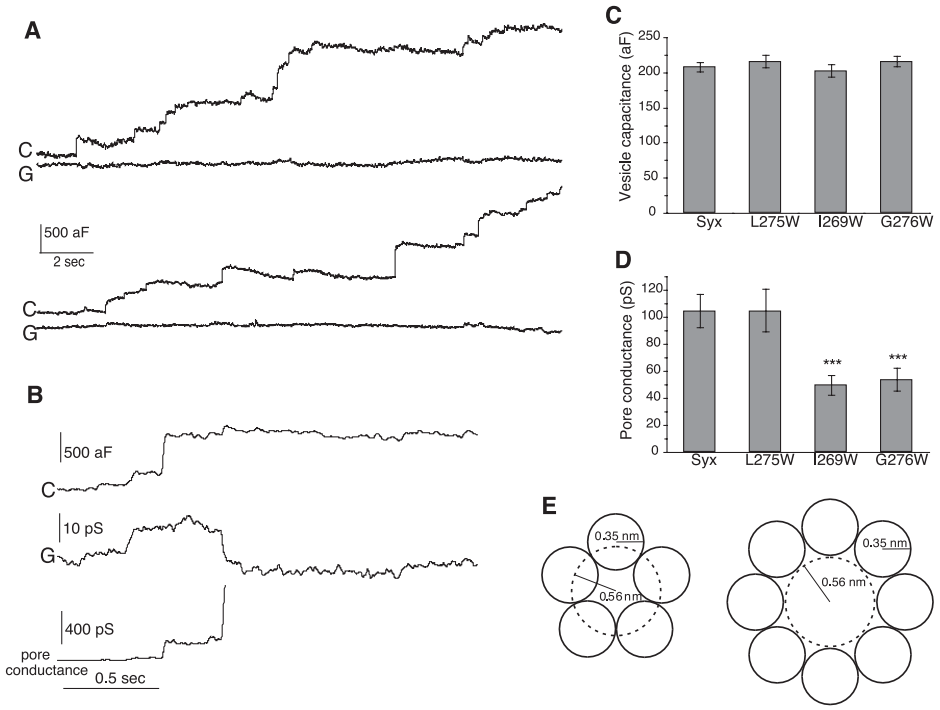

Fig. 4. Capacitance steps and fusion-pore conductance in cell-attached patches of PC12 cells. (**A**) Examples of recordings from two different patches show upward steps in capacitance (C) with no changes in conductance (G). (**B**) Expanding the time scale reveals small deflections in the conductance trace that can be used to compute the fusion-pore conductance as $g_f = (G^2 + C^2)/G$ (*3*). (**C**) Mean step size in capacitance traces for Syx and mutants (N = 503 to 696). (**D**) Mean fusion-pore conductance for Syx and mutants (N = 38 to 60). ***, $P < 0.001$. Error bars show the mean ± SEM. (**E**) Model of a pore with a 0.56-nm radius (dashed circle). Five α helices (0.35-nm radius) (solid circles) can be arranged with the pore edge slightly outside the points of contact (left) (*32*). Eight α helices can be arranged with the pore edge slightly inside the innermost points (right). Solving for the number of helical segments gave 5.62 and 7.96 for circles formed by the points of contact and the inscribed circle, respectively.

thus envision the part of the pore that traverses the plasma membrane as a barrel formed by several copies of the transmembrane segment of Syx, arranged in parallel to form a complete circle (Fig. 4E). It is also possible that other molecules, either protein or lipid, intercalate between the Syx segments to complete the pore structure. Other molecules could provide a connection to the extracellular fluid if the C terminus of Syx remains buried in the membrane (*27*) even after the fusion pore opens. Although the present results provide no direct evidence regarding the participation of other proteins, the observation that the synaptic SNARE proteins, Syx, SNAP-25, and synaptobrevin/vesicle-associated membrane protein (VAMP) constitute a minimal machine for liposome fusion (*23*) suggests that Syx may be the only molecular component of the fusion pore in the plasma membrane. Extrapolating the present results to the vesicle membrane suggests that the transmembrane segment of synaptobrevin/VAMP forms the complementary fusion-pore structure through the vesicle membrane, and that the SNARE complex holds these two parts together. The SNARE complex would then have to form at some point before the fusion pore opens and neurotransmitters are released (*28*, *29*).

The cooperative participation of SNARE complexes in fusion (*30*, *31*) supports the idea that fusion pores are formed from multiple copies of Syx. With a barrel of Syx transmembrane segments as the minimal structure, we constructed a simple model of the plasma membrane side of the fusion pore (Fig. 4E). This model yielded copy numbers ranging from 5 to 8 depending on whether we used the contact points (Fig. 4E, left) or innermost points (Fig. 4E, right) of the transmembrane segments, respectively (*32*). The inclusion of other molecules in the pore structure could reduce the number of participating Syx molecules. Variations in fusion-pore size (*6*, *7*, *11*) could reflect different molecular partners or different numbers of Syx transmembrane segments.

Because fusion-pore opening and dilation constitute critical steps in exocytosis, hypotheses for regulation by Ca^{2+} require that a Ca^{2+} sensor targets the proteins that form the fusion pore. The modulation of these steps by synaptotagmin, the putative Ca^{2+} sensor of exocytosis, therefore requires interactions with fusion-pore proteins. This indicates that the regulation of fusion-pore stability by synaptotagmin (*10*, *11*) is likely to be mediated by Ca^{2+}-promoted binding to SNAREs or SNARE complexes (*12*, *13*).

References and Notes

1. E. Neher, A. Marty, *Proc. Natl. Acad. Sci. U.S.A.* **79**, 6712 (1982).
2. L. J. Breckenridge, W. Almers, *Nature* **328**, 814 (1987).
3. K. Lollike, N. Borregaard, M. Lindau, *J. Cell Biol.* **129**, 99 (1995).
4. R. H. Chow, L. von Rüden, E. Neher, *Nature* **356**, 60 (1992).
5. G. Alvarez de Toledo, R. Fernandez-Chacon, J. M. Fernandez, *Nature* **363**, 554 (1993).
6. M. Lindau, W. Almers, *Curr. Opin. Neurobiol.* **7**, 509 (1995).
7. V. A. Klyachko, M. B. Jackson, *Nature* **418**, 89 (2002).
8. E. Ales *et al.*, *Nature Cell Biol.* **1**, 40 (1999).
9. J. B. Sorensen *et al.*, *Cell* **114**, 75 (2003).
10. C.-T. Wang *et al.*, *Science* **294**, 1111 (2001).
11. C.-T. Wang *et al.*, *Nature* **424**, 943 (2003).
12. J. Bai, C.-T. Wang, D. A. Richard, M. B. Jackson, E. R. Chapman, *Neuron* **41**, 929 (2004).
13. E. R. Chapman, *Nature Rev. Mol. Cell Biol.* **3**, 498 (2002).
14. E. Neher, *Neuroscience* **26**, 727 (1988).
15. B. Hille, *Neuron* **9**, 187 (1992).
16. G. P. Ahern, V. A. Klyachko, M. B. Jackson, *Trends Neurosci.* **25**, 510 (2002).
17. K. Imoto *et al.*, *Nature* **335**, 645 (1988).
18. H. A. Lester, *Annu. Rev. Biophys. Biomol. Struct.* **21**, 267 (1992).
19. K. L. Schulze, K. Broadie, M. S. Perin, H. J. Bellen, *Cell* **80**, 311 (1995).
20. J. Blasi *et al.*, *EMBO J.* **12**, 4821 (1993).
21. R. Jahn, T. C. Südhof, *Annu. Rev. Biochem.* **68**, 863 (1999).
22. R. C. Lin, R. H. Scheller, *Annu. Rev. Cell Dev. Biol.* **16**, 19 (2000).
23. T. Weber *et al.*, *Cell* **92**, 759 (1998).
24. Additional information is available as supporting material on *Science* Online.
25. Single-letter abbreviations for the amino acid residues are as follows: A, Ala; C, Cys; D, Asp; E, Glu; F, Phe; G, Gly; H, His; I, Ile; K, Lys; L, Leu; M, Met; N, Asn; P, Pro; Q, Gln; R, Arg; S, Ser; T, Thr; V, Val; W, Trp; and Y, Tyr.
26. T. L. Colliver, E. J. Hess, E. N. Pothos, D. Sulzer, A. G. Ewing, *J. Neurochem.* **74**, 1086 (2000).
27. K. Suga, T. Yamamori, K. Akagawa, *J. Biochem.* **133**, 325 (2003).
28. Y. A. Chen, S. J. Scales, S. M. Patel, Y.-C. Doung, R. H. Scheller, *Cell* **97**, 165 (1999).
29. Z. Xia, Q. Zhou, J. Lin, Y. Liu, *J. Biol. Chem.* **276**, 1766 (2001).
30. B. A. Stewart, M. Mohtashami, W. S. Trimble, G. L. Boulianne, *Proc. Natl. Acad. Sci. U.S.A.* **97**, 13955 (2000).
31. Y. Hua, R. H. Scheller, *Proc. Natl. Acad. Sci. U.S.A.* **98**, 8065 (2001).
32. We used a simple formula for channel conductance: $\gamma = A/\rho l$ (*33*). γ was taken as 100 pS from our measurement for wild-type Syx (Fig. 4D). ρ is the resistivity of the pore lumen (100 ohm·cm), A is the area, and l is the length. $l \sim 10$ nm because it spans two lipid bilayers. Solving for A gave 1 nm^2. This gives a circle radius of 0.56 nm. If each transmembrane segment is an α helix with a radius of 0.35 nm, we can arrange 5 to 6 segments in a circle for which the points of contact form a circle with a 0.56-nm radius (Fig. 4E, left), or 8 segments for which the innermost points form a circle with a 0.56-nm radius (Fig. 4E, right).
33. B. Hille, *Ion Channels of Excitable Membranes* (Sinauer, Sunderland, MA, ed. 2, 1992).

34. We thank P. Chang for computer programs and V. Klyachko for help with capacitance measurements. This study was supported by NIH (NS30016 and NS44057 to M.B.J. and GM56827 and MH61876 to E.R.C.) and the Milwaukee Foundation (E.R.C.). E.R.C. is a Pew Scholar in the Biomedical Sciences. J.B. was an AHA Predoctoral Fellow.

Supporting Online Material
www.sciencemag.org/cgi/content/full/1095801/DC1
SOM Text
References and Notes

20 January 2004; accepted 1 March 2004
Published online 11 March 2004;
10.1126/science.1095801
Include this information when citing this paper.

Protection from Cardiac Arrhythmia Through Ryanodine Receptor–Stabilizing Protein Calstabin2

Xander H. T. Wehrens,[1,2]* Stephan E. Lehnart,[1,2]* Steven R. Reiken,[1,2] Shi-Xian Deng,[3] John A. Vest,[1,2,3] Daniel Cervantes,[3] James Coromilas,[3] Donald W. Landry,[3] Andrew R. Marks[1,2,3]†

Ventricular arrhythmias can cause sudden cardiac death (SCD) in patients with normal hearts and in those with underlying disease such as heart failure. In animals with heart failure and in patients with inherited forms of exercise-induced SCD, depletion of the channel-stabilizing protein calstabin2 (FKBP12.6) from the ryanodine receptor–calcium release channel (RyR2) complex causes an intracellular Ca^{2+} leak that can trigger fatal cardiac arrhythmias. A derivative of 1,4-benzothiazepine (JTV519) increased the affinity of calstabin2 for RyR2, which stabilized the closed state of RyR2 and prevented the Ca^{2+} leak that triggers arrhythmias. Thus, enhancing the binding of calstabin2 to RyR2 may be a therapeutic strategy for common ventricular arrhythmias.

Ventricular tachyarrhythmias that cause SCD are often associated with common heart diseases, such as heart failure, but may also occur in individuals without structural heart disease (*1*). Treatment remains largely empirical, in part because of an incomplete understanding of the underlying cellular mechanisms that trigger the arrhythmias (*2*). RyR2 is required for Ca^{2+} release from the sarcoplasmic reticulum (SR) during systole, when activation of heart muscle contraction occurs. During the resting phase of the cardiac cycle (diastole), binding of calstabin2 (also known as the FK506-binding protein, FKBP12.6) to RyR2 helps maintain the channel in a closed state to prevent leakage of SR Ca^{2+} into the cytoplasm (*3*, *4*). In heart failure (*5*) and catecholaminergic polymorphic ventricular tachycardia (an inherited form of exercise-